5-2020

Monte Carlo Simulations of Ultracold Neutron Velocities

Isaiah Cox

MONTE CARLO SIMULATIONS OF ULTRACOLD NEUTRON VELOCITIES

Isaiah Cox

A Thesis Submitted in Partial Fulfillment of the Requirements for the ETSU Honors in Discipline Program

April 2020

Author: _____

Isaiah Cox Date

Mentor: _____

Robert W. Pattie, Ph.D. Date

Reader: _____

Gary D. Henson, Ph.D. Date

Abstract

An electric dipole moment (EDM) in the neutron would indicate a source of CP-violation that is needed to explain the dominance of matter over antimatter in the universe. Several experiments are currently looking for a neutron EDM and so far, the value has been constrained to $d_n < 1.8 \times 10^{-26} e{\cdot}\text{cm}$. Presented here is work supporting the nEDM experiment at Los Alamos National Laboratory which utilizes ultracold neutrons (UCNs) and Ramsey's separated oscillating fields method. In such an experiment, it is important to understand the velocity of the neutrons due to false EDM signals that can be produced by the presence of a magnetic field. Monte Carlo simulations were used to study the optimal design parameters of a chopper system that would reproduce a given velocity spectrum of a population of neutrons by measuring the time of flight to a detector.

1 Introduction

High energy physics is used to discover new particles of very high mass. A particle of mass M can be produced if the energy in a reaction exceeds $7Mc^2$. The unification of the electromagnetic and weak forces was discovered in this way by colliding protons at energies in the TeV range. These reactions produce the Z^0 and $W^{\pm}$ bosons that communicate the weak force (Kenyon, 1985).

If we are looking for a particle whose mass is greater than the energies available to us in accelerators, then we use Heisenberg's uncertainty principle to look for virtual particles. The probability of these virtual particles appearing is given by a propagator where

$$\text{propagator} \propto \frac{1}{\left(\frac{p}{c}\right)^2 - M^2}. \tag{1}$$

In the really interesting cases, where $M^2 >> (p/c)^2$, we have

$$\text{propagator} \propto \frac{1}{M^2} \tag{2}$$

which does not depend on reaction energy. We can write

$$M^2 \sim \frac{v^2}{\sigma} \sim \frac{2\sqrt{2}}{G_F \sigma} \sim \frac{174\text{GeV}}{\sigma} \tag{3}$$

where G_F is the Fermi coupling constant and σ is the precision of the experiment. Thus, a $\sigma = 0.01\%$ measurement of a fundamental parameter corresponds to a mass scale of 17.4TeV. For this reason, precision measurements allow us to probe higher energy scales than direct measurements in particle accelerators.

Working with low energy neutrons provides very precise measures of some important quantities such as changes in energy, momentum, and spin. Often times, these small changes violate some fundamental symmetry which is of great interest in many areas of science.

For example, cosmologists are trying understand the process that led to the dominance of matter over antimatter in the universe. It is predicted by current theories that the amount of matter created should be the same as the amount of antimatter, and we should be left with a universe made up almost entirely of energy. That is, the ratio of baryons and antibaryons to photons should be (Dubbers and Schmidt, 2011)

$$\frac{n_b}{n_\gamma} = \frac{n_{\bar{b}}}{n_\gamma} \sim 10^{-18}. \tag{4}$$

However, observation (Spergel et al., 2003) tells us that $n_{\bar{b}} \approx 0$ and

$$\frac{n_b}{n_\gamma} \approx 10^{-10}. \tag{5}$$

Three necessary conditions have been identified for such a scenario to occur. These conditions are referred to collectively as the Sakharov criteria (Sakharov, 1967). They are

as follows:

1. Baryon number violation

2. Charge (C) and Charge-Parity (CP) symmetry violation

3. Thermal non-equilibrium

It is the second condition, the violation of CP symmetry, in which low energy neutron experiments can be of help.

If the neutron has a permanent non-zero electric dipole moment (EDM), then that would be a source of CP symmetry violation. Note that the neutron has a magnetic dipole moment of $\mu_n = -0.603 \times 10^{-7}$ eV/T. The spin precession about an external field $\mathbf{B}$ is given by

$$\dot{\mathbf{P}} = \boldsymbol{\omega}_0 \times \mathbf{P}, \tag{6}$$

where $\mathbf{P} = \langle \mathbf{j} \rangle / \hbar j$ is the polarization vector and the precession frequency vector is $\boldsymbol{\omega}_0 = \frac{\mu_n \mathbf{B}}{j\hbar} = \gamma_n \mathbf{B}$. The gyromagnetic ratio of the neutron is $\gamma_n / 2\pi = 29.16$ MHz/T.

If the neutron also has an EDM, $\mathbf{d}$, then it too would be coupled with the spin operator as $\mathbf{d} = d\boldsymbol{j}$. When an external electric field is applied, the precession frequency vector would then be

$$\boldsymbol{\omega}_+ = \frac{2(\mu_n \mathbf{B} + d\mathbf{E})}{\hbar}. \tag{7}$$

Here, we can see how an EDM violates P symmetry. Since $\mathbf{E}$ is a vector, it changes sign. However, $\mathbf{B}$ is a pseudovector so its direction is unchanged under parity transformations. That is $P : \mathbf{E} \to -\mathbf{E}$, $P : \mathbf{B} \to \mathbf{B}$, and $P : \mathbf{j} \to \mathbf{j}$. Thus, we have

$$P : \boldsymbol{\omega}_+ \to \boldsymbol{\omega}_- = \frac{2(\mu_n \mathbf{B} - d\mathbf{E})}{\hbar} \tag{8}$$

Under a time reversal (T) transformation, pseudovectors change direction while vectors re-

main unchanged so $T : \mathbf{E} \to \mathbf{E}$, $T : \mathbf{B} \to -\mathbf{B}$, and $T : \mathbf{j} \to -\mathbf{j}$. Thus,

$$T : \boldsymbol{\omega}_+ \to \boldsymbol{\omega}_- = \frac{-2(-\mu_n \mathbf{B} + d\mathbf{E})}{\hbar} = \frac{2(\mu_n \mathbf{B} - d\mathbf{E})}{\hbar}. \tag{9}$$

Therefore, a neutron EDM violates P and T symmetry. Futhermore, under the CPT theorem, which assumes the invariance of CPT transformations, a violation of T symmetry is equivalent to a violation of CP symmetry.

Currently, there are several nEDM experiments utilizing ultracold neutrons including those at Los Alamos and Oak Ridge National Labs in the US, as well as TRIUMF, PSI, and ILL internationally (Dubbers and Schmidt, 2011). Ultracold neutrons (UCN) are useful in nEDM searches due to their ability to be stored for long periods of time. This is because they have velocities lower than the critical velocity $v_c = \sqrt{2V/m}$ determined by the effective potential, V, of the surface of the container. This potential is given by

$$V = \frac{2\pi\hbar^2}{m_n}\mathcal{N}b, \tag{10}$$

where $\mathcal{N}$ is the nucleon density of the material and b is the neutron scattering length (Schmidt-Wellenburg, 2016). The kinetic energy of a neutron perpendicular to the surface of the container is given by

$$E_\perp = \frac{(\hbar k \sin(\theta))^2}{2m_n} \tag{11}$$

where k is the wavenumber. If $E_\perp < V$, then the neutron will be totally reflected. Furthermore, the reflection is specular assuming the scattering is elastic (Cubitt and Fragneto, 2002).

To measure the EDM of a neutron, we measure the precession frequency in an electric field $\mathbf{E}$. However, this is not practical because the precession frequency caused by the interaction between the magnetic moment and an external $\mathbf{B}$ field will cause a much larger precession frequency than the one we are actually trying to measure. Since there is no way to shield the experiment from magnetic fields well enough, we simply measure the difference

in precession frequency with the **E** field parallel to **B** (ω_+) and antiparallel (ω_-). Then, we have (Schmidt-Wellenburg, 2016)

$$d_n = \frac{\hbar(\omega_+ - \omega_-) - 2\mu_n(B_+ - B_-)}{2(E_+ - E_-)}. \tag{12}$$

Ramsey's method is one way to make this measurement. This method involves applying a $\pi/2$ flip to a population of polarized neutrons exposed to a magnetic field B_0. The neutrons precess freely with their spin perpendicular to the magnetic field for a time T. During this time, their rotation gains a phase of $\phi = 2d_nE_zT/\hbar$ if $d_n \neq 0$. Then, a second $\pi/2$ flip will produce a polarization of $P_z \approx -\phi$ if the initial polarization was $P_{z0} = 1$.

For a large number of neutrons $N \gg 1$, a spin analyzer will transmit $N_+ \approx \frac{N}{2}(1+\phi)$ when it is oriented parallel to the z axis and $N_- \approx \frac{N}{2}(1-\phi)$ when oriented antiparallel. Thus, we have

$$\phi \pm \Delta\phi = \frac{N_+ - N_-}{N} \pm \frac{1}{\sqrt{N}}. \tag{13}$$

Now, we can calculate the measured EDM with its uncertainty as

$$d_n \pm \Delta d_n = \frac{(N_+ - N_-)\hbar}{2E_zTN} \pm \frac{\hbar}{2E_zT\sqrt{N}}. \tag{14}$$

We would like Δd_n to be as small as possible so the goal is to maximize $E_zT\sqrt{N}$. Free neutrons decay so T is limited by the neutron lifetime which is around 880s. The electric field can in principle be large, however, leakage currents cause magnetic fields that affect the measurement so E_z must be low enough to avoid this. Furthermore, the breakdown of a high electric field can damage the electrode surface. Therefore, increasing N is the best way to improve experiment sensitivity (Dubbers and Schmidt, 2011).

It is important to understand all of the systematic effects that are present in such a design. For example, the inhomogeneity of the magnetic field can lead to a false EDM signal that is important for experiments with sensitivities on the scale of 10^{-28} e·cm. This signal comes from the geometric phases induced by the neutron experiencing a time dependent magnetic

field from its reference frame (Pendlebury et al., 2004). As the magnetic field changes direction, the neutron's magnetic moment picks up an extra geometric phase $\gamma = \frac{1}{2}\Omega$ in a time T, where Ω is the solid angle that $\mathbf{B}$ sweeps through. We can approximate the motion of the neutrons as along a horizontal circle of radius r and angular frequency ω_r. The motion is perpendicular to $\mathbf{B}$ but if there is some $\mathbf{B}_\perp$ component that is constant along the neutron's trajectory, then we have

$$\Omega \approx \pi \frac{B_\perp^2}{B^2}.$$

The geometric phase builds up after n path orbits to $n\gamma = (\omega_r T/2\pi)\cdot\frac{1}{2}\Omega$. However, this effect is independent of $\mathbf{E}$ so it would cancel in the EDM experiment when the field is switched. The problem comes from the magnetic field induced by the velocity of the neutrons given by

$$\mathbf{B}_v = \frac{\mathbf{v}\times\mathbf{E}}{c^2} \tag{15}$$

which is in the same direction as $\mathbf{B}_\perp$. Now the geometric phase becomes

$$\gamma \approx \frac{1}{2}\pi\frac{(\mathbf{B}_\perp + \mathbf{B}_v)^2}{B^2} = \frac{1}{2}\pi\frac{\mathbf{B}_\perp^2 + 2\mathbf{B}_\perp\cdot\mathbf{B}_v + \mathbf{B}_v^2}{B^2}. \tag{16}$$

Since $2\mathbf{B}_\perp\cdot\mathbf{B}_v$ depends on $\mathbf{E}$, the phase doesn't cancel so we measure a false EDM signal from $n\gamma = (B_\perp B_v/2B^2)\omega_r T$.

To date, a neutron EDM has not been observed. Currently, the best upper limit has come from the nEDM experiment at the Paul Scherrer Institute in Switzerland. They have constrained the value to be $d_n < 1.8\times10^{-26} e\cdot$cm (Abel et al., 2020) which represents an improvement of six orders of magnitude over the inital measurement of $d_n < 5\times10^{-20} e\cdot$cm made by Smith, Purcell, and Ramsey, 1957. The nEDM experiment at LANL hopes to improve this result by a factor of 10 (Clayton et al., 2017), while ORNL hopes to use the spallation neutron source to improve it by a factor of 100 (Collaboration et al., 2007).

2 Monte Carlo Simulations

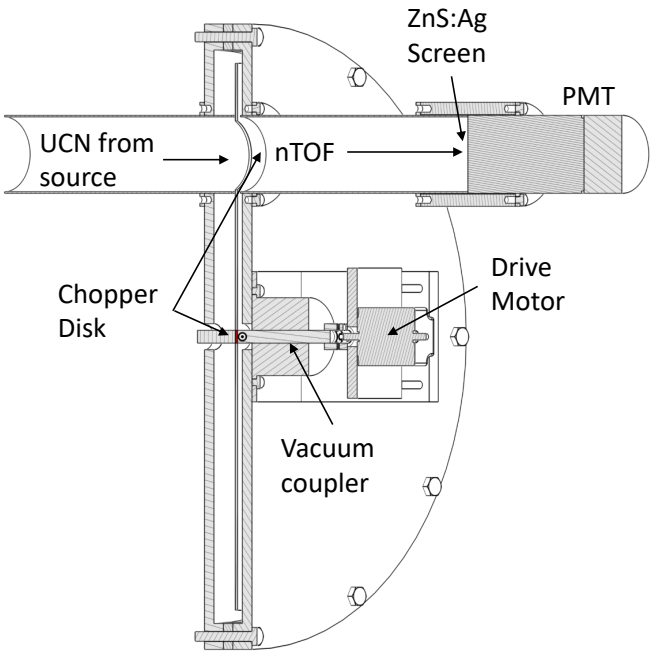

Figure 1: Neutrons enter from the left and are allowed to pass through to the detector when the chopper is open.

2.1 Time of Flight

Due to the velocity dependence of the effect described in the previous section, it is important to know the velocity spectrum of the neutrons in the experiment. Time of flight (TOF) techniques can be used to measure the velocity distribution of the neutrons coming from the source. One such method involves the use of a chopper system that is capable of producing a population of neutrons all starting at the same time and distance from a detector as shown in Figure 1. In this setup, an opening is cut into a disk which rotates through the beam in which the neutrons are traveling. When the opening passes through the beam, neutrons are allowed to pass through, to be detected a distance ℓ away. Due to the different neutron

velocities, the amount of time the neutrons require to reach the detector will vary. This gives an estimate of the velocity along the axis of the chopper and detector.

The goal of this study is to provide Monte Carlo simulation results for various chopper system designs to determine what parameters will best reproduce the given velocity distribution. This information will then be used in the design and construction of a spectrometer supporting the nEDM experiment at Los Alamos National Laboratory. In the simulations performed, the chopper system is placed off of the north beamline going towards the nEDM experiment. The layout of the exeriment hall at Los Alamos is shown in Figure 2.

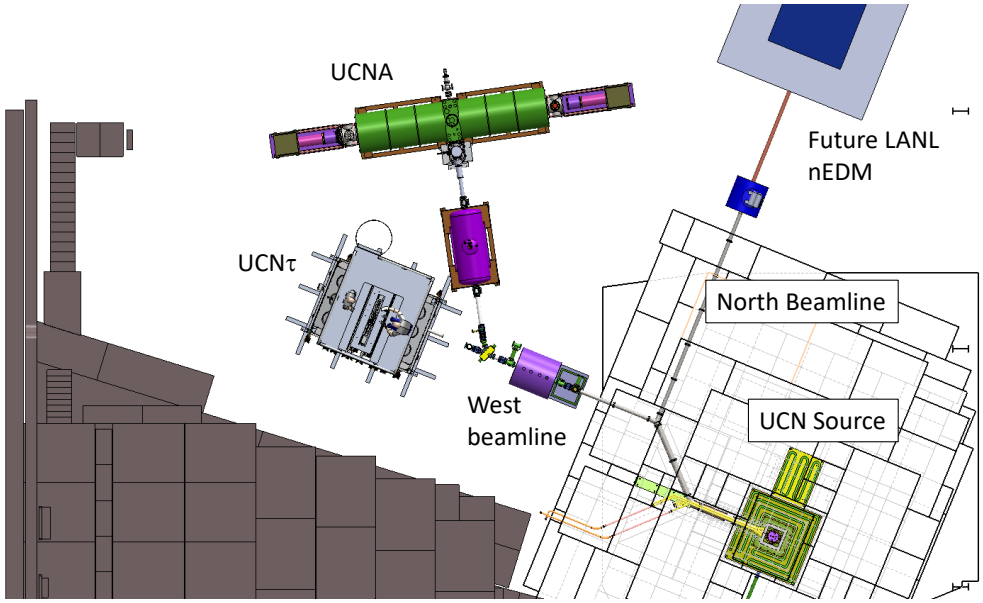

Figure 2: Area B at LANL houses several UCN experiments including nEDM.

2.2 Simulation Parameters

In the simulation, neutrons are created with random velocities according to a Maxwell-Boltzmann distribution. A geometry file is used to create the parameters of the chopper system. The system is placed just off of the main transport tube and neutrons are

created in the volume with the chopper. The chopper is placed at the edge of this volume and a separate volume is created with the detector. One parameter we are interested in is the distance from the chopper to the detector, ℓ. Simulations are performed for $\ell = \{0.10\text{m}, 0.20\text{m}, 0.30\text{m}, 0.40\text{m}, 0.50\text{m}\}$.

The neutrons are produced in bursts 10 times during each simulation and the chopper is opened and neutrons are allowed to enter the volume of the detector a total of 10 times as well. Other parameters we are interested in are the length of time the chopper remains open, Δt, and the delay from the beam pulse, dt. Simulations were performed for $\Delta t = \{0.01\text{s}, 0.07\text{s}, 0.13\text{s}, 0.19\text{s}, 0.25\text{s}\}$ and $dt = \{0.00\text{s}, 0.25\text{s}, 0.50\text{s}, 0.75\text{s}, 1.00\text{s}\}$.

The final parameter we are looking at is the absorption of the chopper. We perform simulations for absorption rates of 0.0 and 1.0. Thus, we perform a total of 250 simulations. The parameters are summarized in Table 1.

Table 1: Simulated parameter values.

Absorption	dt(s)	Δt(s)	ℓ(m)
0.0	0.00	0.01	0.10
1.0	0.25	0.07	0.20
	0.50	0.13	0.30
	0.75	0.19	0.40
	1.00	0.25	0.50

2.3 Comparison

The results of the simulations are stored in ROOT files. The information includes the initial speed of the particles as well as the time of flight to the detector. This allows us to compare the velocity spectrum that we would calculate with the detector to the actual velocity spectrum. A (*Kolmogorov–Smirnov*) KS test is used to determine which simulation produces the best time of flight histogram that would allow us to accurately measure the velocity spectrum of the neutrons.

The KS test is used to measure the similarity of two different cumulative distribution functions. The test statistic is given by

$$D = max\,|F_o(X) - F_r(X)| \tag{17}$$

where F_o is the calculated cumulative frequency distribution and F_r is the actual distribution. The simulation with the lowest value for D, corresponding to higher p-values, will provide us with information on the optimal parameters for our chopper system.

3 Results and Discussion

The simulations that best reproduce the initial velocity spectrum have longer flight distances and zero absorption. The simulation with the highest p-value from the KS test has the parameters shown in Table 2. The time of flight and velocity histograms for this simulation

Table 2: Parameter values of the best reproduction.

Absorption	dt(s)	Δt(s)	ℓ(m)
0.0	0.75	0.07	0.400

are shown in Figure 3. The top left plot shows the number of particles with a given time of flight. The spikes every 5 seconds are a result of the chopper openings, thus allowing a new population of neutrons to begin traveling to the detector. In the remaining histograms, the time of flight is reduced modulo 5 so that the value is the time after the chopper was open. This improves statistics, however the number of neutrons that overlap between opening can introduce error. The top center plot is a 2D histogram showing the initial speed and the time of flight. The color bar represents the number of neutrons with a given initial speed and time of flight. The top right plot is similar but with initial velocity in the direction towards the detector instead of speed. The bottom left shows the number of neutrons with a given

initial speed and the number of neutrons with a given calculated speed. These histograms are isolated in Figures 4 and 5. The bottom center shows the number of neutrons with a given initial velocity towards the detector that got detected. The different colors represent different flight times. It makes sense that neutrons with higher velocities towards the detector will be detected more often than those with lower velocities. The smaller peaks are likely those neutrons which are left over from the previous opening of the chopper, since this calculation uses the absolute time of flights rather than the reduced. The bottom right plot simplifies the top right by averaging the velocity towards the detector for a given time of flight bin.

The normalized input speed and calculated speed counts are shown in Figures 4 and 5. Since the system can really only measure the velocity towards the detector, it makes sense that the calculated speed underestimates the true speed. A better understanding of this effect can allow for corrections to the measurements.

The cumulative distribution functions for the input and calculated speeds are shown in Figure 6. Again, it is obvious that the calculated speed for most neutrons is less than the true speed since only those with velocities towards the detector when the chopper is opened will be accurately measured.

In total, 35 of the 250 simulations had p-values greater than 0.50. These parameters are shown in Table 3. As can be seen, none of these simulations has an absorption of 1.00 or a flight distance $\ell < 0.400$. Furthermore, all of these have some delay between the beam pulse and the time when the chopper opens.

Since each simulation started with 5 million neutrons, some configurations end up with a much higher number of neutrons making it to the detector. This is certainly the case with the absorption parameter of the chopper. When the chopper is perfectly absorbing, less than 0.5%, around 10^4 neutrons, make it to the detector. On the other hand when the absorption is 0.00, around 6% of neutrons generally make it to the detector, which is more than a factor of 10 increase. Another factor that may affect the efficiency is the flight length. For $\ell = 0.100$m and zero absorption, as many as 30% of the neutrons make it to the detector. However, this is possibly a bug in the code as not all $\ell = 0.100$m cases exhibit this behavior.

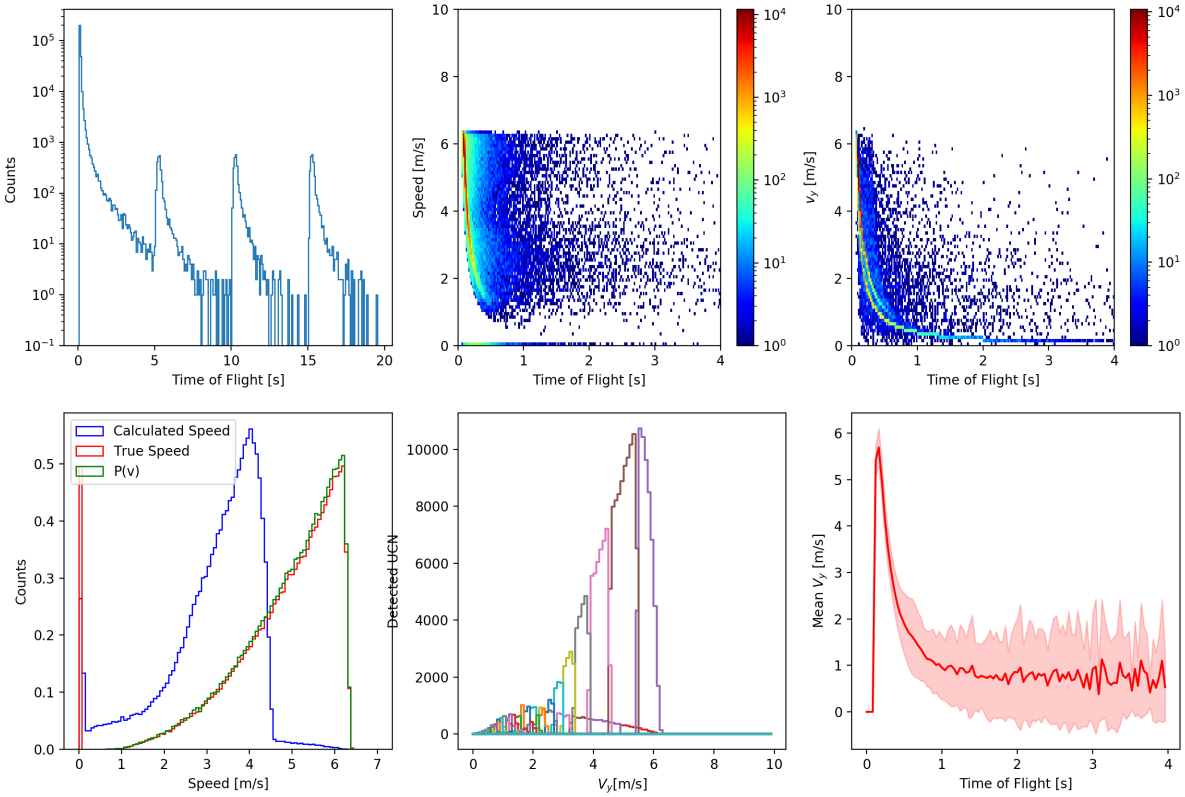

Figure 3: Histograms for the simulation with parameters shown in Table 1.

4 Conclusions

Here we have discussed the importance of understanding the velocity spectrum of the neutron population in EDM experiments. We have presented the results of simulations to determine the optimal parameters of a chopper system designed to measure the velocity spectrum of neutrons. Further analysis of these results is required to better understand the parameter space. Also, new simulations should be performed taking advantage of the information provided here that shows longer flight paths and non-absorbing chopper material yield better results. With these constraints, the parameter space can be explored with higher resolution.

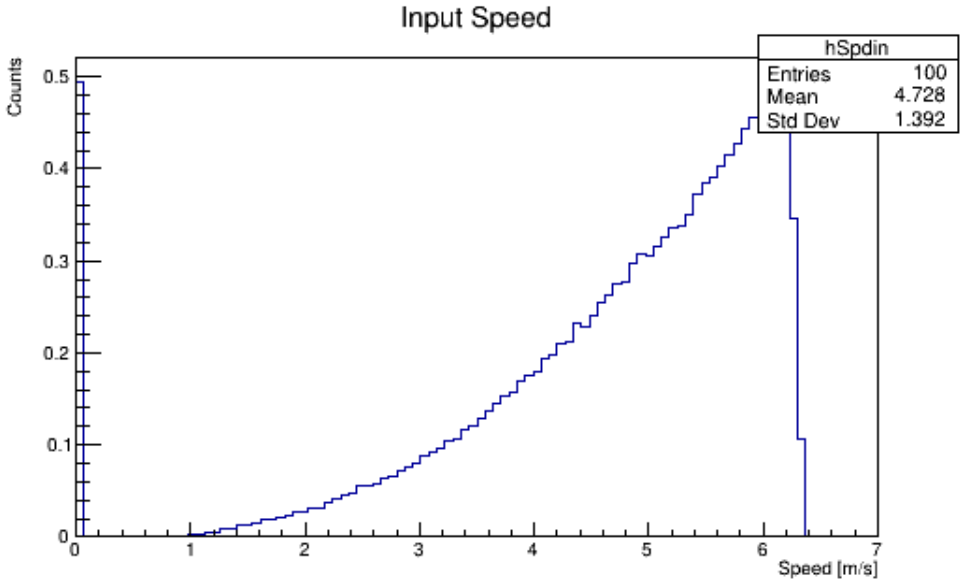

Figure 4: Histogram showing the initial speeds.

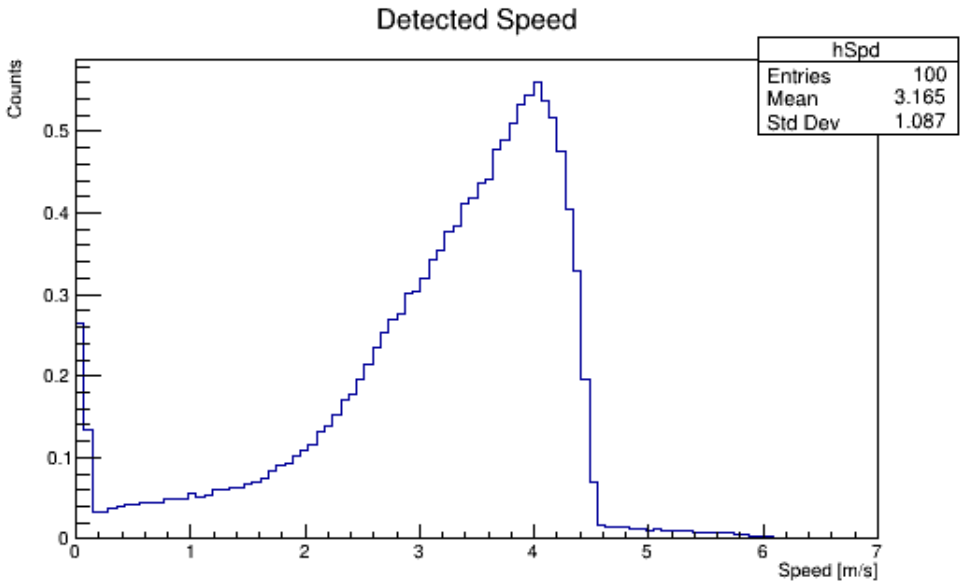

Figure 5: Histogram showing the calculated speeds.

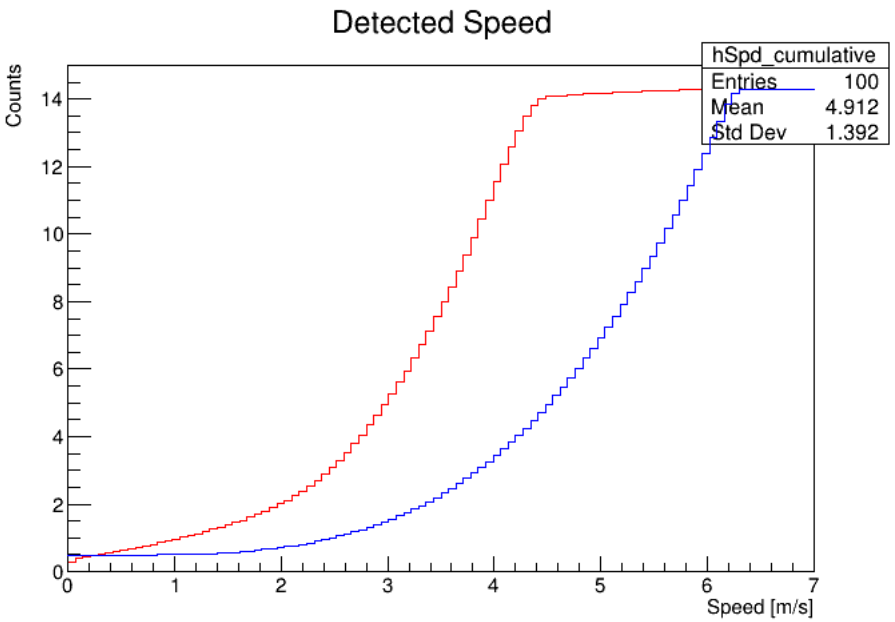

Figure 6: Cumulative distribution functions of the initial speed (blue) and the calculated speed (red).

Table 3: Parameter values of the 35 best reproductions.

Absorption	dt(s)	Δt(s)	ℓ(m)
0.0	1.00	0.07	0.500
0.0	0.50	0.13	0.500
0.0	0.50	0.25	0.500
0.0	0.25	0.25	0.500
0.0	0.25	0.25	0.400
0.0	0.75	0.19	0.400
0.0	0.50	0.25	0.400
0.0	0.75	0.19	0.500
0.0	1.00	0.13	0.400
0.0	0.25	0.07	0.400
0.0	0.50	0.07	0.500
0.0	1.00	0.01	0.400
0.0	0.75	0.13	0.500
0.0	0.25	0.19	0.500
0.0	1.00	0.13	0.500
0.0	0.50	0.19	0.500
0.0	1.00	0.07	0.400
0.0	0.50	0.01	0.400
0.0	0.75	0.07	0.500
0.0	1.00	0.25	0.500
0.0	0.25	0.13	0.400
0.0	0.25	0.01	0.400
0.0	1.00	0.19	0.500
0.0	0.75	0.01	0.400
0.0	0.75	0.01	0.500
0.0	0.50	0.13	0.400
0.0	1.00	0.01	0.500
0.0	0.75	0.25	0.400
0.0	0.75	0.07	0.400
0.0	1.00	0.19	0.400
0.0	0.50	0.01	0.500
0.0	0.75	0.25	0.500
0.0	0.50	0.19	0.400
0.0	1.00	0.25	0.400
0.0	0.75	0.13	0.400

References

[1] I Kenyon. "The discovery of the intermediate vector bosons". In: *European Journal of Physics* 6.1 (1985), p. 41.

[2] Dirk Dubbers and Michael G Schmidt. "The neutron and its role in cosmology and particle physics". In: *Reviews of Modern Physics* 83.4 (2011), p. 1111.

[3] D. N. Spergel et al. "First-Year Wilkinson Microwave Anisotropy Probe (WMAP) Observations: Determination of Cosmological Parameters". In: 148.1 (Sept. 2003), pp. 175–194. DOI: 10.1086/377226. arXiv: astro-ph/0302209 [astro-ph].

[4] Andrej Dmitrievich Sakharov. "Violation of CP invariance, C asymmetry, and baryon asymmetry of the universe". In: *JETP lett.* 5 (1967), pp. 24–27.

[5] P Schmidt-Wellenburg. "The quest to find an electric dipole moment of the neutron". In: *arXiv preprint arXiv:1607.06609* (2016).

[6] R Cubitt and G Fragneto. *Neutron Reflection: Principles and Examples of Applications, Chapter 2.8. 3 of book" Scattering" edited by R. Pike and P. Sabatier*. 2002.

[7] JM Pendlebury et al. "Geometric-phase-induced false electric dipole moment signals for particles in traps". In: *Physical Review A* 70.3 (2004), p. 032102.

[8] Christopher Abel et al. "Measurement of the permanent electric dipole moment of the neutron". In: *Physical Review Letters* 124.8 (2020), p. 081803.

[9] JH Smith, EM Purcell, and NF Ramsey. "Experimental limit to the electric dipole moment of the neutron". In: *Physical Review* 108.1 (1957), p. 120.

[10] Steven Clayton et al. "Los Alamos nEDM Experiment and Demonstration of Ramsey's Method on Stored UCNs at the LANL UCN Source". In: *APS* 2017 (2017), CG–003.

[11] nEDM Collaboration et al. "Conceptual design report for the neutron electric dipole moment project (nEDM)". In: *Prepared for the US Dept. of Energy Office of Nuclear Physics* (2007).